

Physics Laboratory 2 for Beginners
Laboratory in Winter Semester 2018/19

Experiment 81: Determination of the Planck constant with the Photoelectric Effect

(carried out on 27. March 2019 under supervision of

)

29. March 2019

Contents

1 Objective	4
2 Theoretical Basis	4
3 Setup and Procedure	6
3.1 Determination of the Wavelengths from the Diodes . . .	6
3.2 Current-Voltage Characteristic of a Diode for Different Intensities	6
3.3 Current-Voltage Characteristic for Different Frequencies and Determination of the reverse voltage	7
4 Measurement	7
4.1 Determination of the Wavelengths from the Diodes . . .	7
4.2 Current-Voltage Characteristic of a Diode for Different Intensities	7
4.3 Current-Voltage Characteristic for Different Frequencies and Determination of the reverse voltage	8
5 Analysis	8
5.1 Determination of the Wavelengths from the Diodes . . .	8
5.2 Current-Voltage Characteristic of a Diode for Different Intensities	9
5.3 Current-Voltage Characteristic for Different Frequencies and Determination of the reverse voltage	11
5.4 Determination of the Planck Constant	15
6 Discussion	17
6.1 Determination of the Wavelengths from the Diodes . . .	17
6.2 Current-Voltage Characteristic of a Diode for Different Intensities	18
6.3 Current-Voltage Characteristic for Different Frequencies and Determination of the reverse voltage	18
6.4 Determination of the Planck Constant	19
A Appendix	20
A.1 Linear Regression	20
A.2 Lab Notes	22

Table 1 shows an overview of the symbols used in this lab report.

Symbol	Meaning
E	Energy
E_e	Energy of an electron within a material
E_F	Fermi energy
E_{kin}	Kinetic energy
h	Planck constant
ν	Frequency
ϕ	Work function
U	Voltage
U_G	Stopping voltage
$U_{G,\text{max}}$	Maximum stopping voltage
I	Intensity, Current
I_{ph}	Photo current
I_V	Current flowing through a voltmeter
r	Distance
R_V	Inner resistance of a voltmeter
e	Elementary charge
c_0	Speed of light
$\aleph, \beth, \beth, \beth$	Parameters of regression
s_x	Error on the (measured) quantity x

Table 1: Symbols used in this lab report

1 Objective

The overall objective of the experiment was to examine the photoelectric effect and determine the planck constant h . By submitting a photocell to light of various wavelengths – which had to be identified prior – the photoelectric effect could be quantified by measuring the photo current. The use of the stopping-field-method allowed the determination of the current-voltage characteristic of the photocell for various wavelengths and intensities of the incoming light. Furthermore, multiple series of measurements were taken to analyze the effect of a current fault circuit or a voltage fault circuit on the current-voltage-characteristic.

2 Theoretical Basis

In the following segment, we will shortly summarize the photoelectric effect. When a cathode gets submitted to the light of an appropriate diode (LED), the photons of the beam of light interact with the electrons on the cathode's surface. By transferring their energy to the electrons, the electrons themselves gain kinetic energy which allow them to exit the cathode. Increasing the intensity of light results in a higher number of photons being emitted and therefore a higher number of electrons leaving the cathode.

This is measurable by placing an anode in a near proximity which attracts the negatively charged electrons.

Within the cathode the electrons exist on different potentials and have therefore different Energies E_e , which are generally limited by the so-called Fermi energy E_F . Therefore, after receiving energy from incoming photons, the electrons kinetic energies differ based on their initial energy in the cathode. By application of a reverse voltage one can limit the electrons reaching the anode. If no photo current is measurable anymore, the maximum kinetic energy of the electrons equals the work done by the electric field.

The energy balance described above can be expressed mathematically. The energy of a photon is

$$E = h\nu, \quad (1)$$

where ν is the frequency of the incoming photon and h the Planck constant. In order to leave the cathode, the electron has to do additional work ϕ depending on the cathode material. The energy balance becomes therefore

$$E_{\text{kin}} = h\nu - \phi - (E_F - E_e), \quad (2)$$

where E_{kin} is the kinetic energy of the electron after exiting the cathode. This kinetic energy has to be matched by the potential energy $e \cdot U_G$ in order to stop incoming electrons. Because the energy E_e is limited by the Fermi energy E_F , no photo current is measurable if

$$h\nu - \phi = eU_{G,\text{max}} \quad (3)$$

holds.

If the cathode and the anode are out of different materials, one has to consider the anode work function¹ ϕ_A :

$$h\nu - \phi_A = e \cdot U_{G,\text{max}}. \quad (4)$$

In order to get from the anode to the cathode, the electron has to have the energy $\phi_A + e \cdot U_G$.

It should be mentioned that the developing photo current is square dependent on the reverse voltage:

$$I_{\text{ph}} \propto (h\nu - \phi - e \cdot U_G)^2. \quad (5)$$

Also, if r is the distance between the light emitting diode and the photo diode, the intensity of light is proportional to the reciprocal of the square of r , in accordance with the inverse-square law:

$$I \propto \frac{1}{r^2} \quad (6)$$

¹In order to maintain simplicity, we will call the anode work function ϕ in the further discussion.

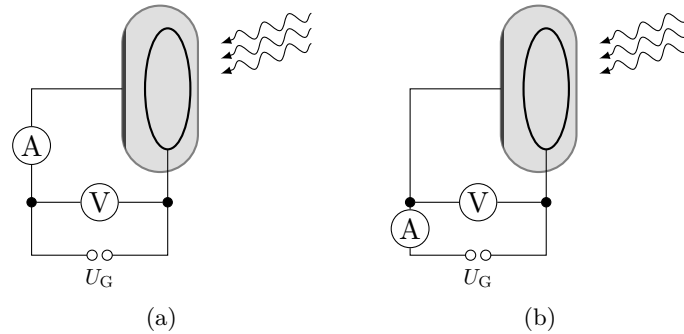


Figure 1: Schematic of a current fault circuit (a) and a voltage fault circuit (b)

3 Setup and Procedure

3.1 Determination of the Wavelengths from the Diodes

In order to determine the wavelengths of the diodes that we used in the following measurements we connected a grating spectrometer to a laptop and opened the program OceanView. The spectrometer was held against the light of a light emitting diode which in turn was connected to a dc generator. OceanView then allowed us to measure the distribution of the intensity of light detected by the spectrometer with respect to the wavelength. The distribution could then be saved to a thumb drive for later analysis.

3.2 Current-Voltage Characteristic of a Diode for Different Intensities

The objective of this part of the experiment was to record the current-voltage-characteristic of a photo diode for different intensities of incoming light. This was done by exposing the photo cell to the light of one specific diode and measuring the photo current of the cell with respect to the cell reverse voltage. Both quantities were measured with separate multimeters as shown in Figure 1a. The photo current was measured for voltages between -4 V and 4 V for three different distances between light emitting diode and photo diode. To compare our measurements by use of the current-fault circuit, we also took a measurement series by using a voltage-fault circuit with a specific distance between diode and photo cell. The circuit is shown in Figure 1b.

3.3 Current-Voltage Characteristic for Different Frequencies and Determination of the reverse voltage

To understand in which way the current-voltage characteristic depends on the frequency of light we recorded five series of measurements of the reverse voltage and the photo current. In each series a different light emitting diode was used. Both the distance between the diodes and the voltage on the LED were deliberately chosen to achieve a photo current of about $50 \mu\text{A}$ for a reverse voltage at around zero.

4 Measurement

All the measurements we took during the experiment can be found in the appendix.

4.1 Determination of the Wavelengths from the Diodes

In order to determine the wavelengths of the light emitting diodes we used the program OceanView as said in section 3.1. The program made it possible for us to see the distribution of the intensity of light w. r. t. its wavelength. To further analyze the intensity distribution, the raw data was saved to a thumb drive. Because the intensity distribution was constantly changing as our hands aren't perfectly steady, it was difficult for us to save the data right in time. Furthermore, while OceanView allows to freeze the intensity distribution momentarily, we haven't found a way to save the "frozen" data. Because the light sensor was saturated for some intensities, we needed a few attempts for saving the data right in time.

4.2 Current-Voltage Characteristic of a Diode for Different Intensities

In order to obtain the current-voltage characteristic of a photo cell we connected a light emitting diode with a dc generator and submitted a photo cell to the light emitted by the diode. Throughout the whole series of measurement the same light emitting diode with a wavelength of $(380 \pm 3) \text{ nm}$ was chosen.

To determine the way the intensity of incoming light influences the photo current, we took three separate series of measurement of the photo current with respect to the stopping voltage for the distances $r = 2.00 \text{ cm}$, 4.00 cm , and 5.50 cm between diode and photo cell, which we measured using a ruler. One can see the results of our measurements in fig. 3.

During our measurement we had to change the range of measurement. The uncertainty of all measured points of voltage with the multimeter is 0.5% of its value + 1 Digit. For the measured current the uncertainty is 2%

of its value + 5 Digits by use of a measuring range of $20 \mu\text{A}$ and 0,8% of its value + 1 Digit by use of a measuring range of $200 \mu\text{A}$.

To compare our measured values we took using the current-fault circuit, we also took one series of measurement using the voltage-fault circuit. In this measurement the distance between diode and photo cell was again 2 cm. The results are evaluated in fig. 4

4.3 Current-Voltage Characteristic for Different Frequencies and Determination of the reverse voltage

To get clear in which way the current-voltage characteristic depends on the frequency of light we recorded five measured series of the reverse voltage and the photo current. We made this series for all in table 2 listed diodes without the diode labeled $(654 \pm 3) \text{ nm}$.

Again we had to change the measuring range in between. The uncertainties arise in the same way as in the part of measurement before.

5 Analysis

5.1 Determination of the Wavelengths from the Diodes

With this measurement we determined the wavelengths of all the diodes we had at our disposal in order to analyze our findings from measuring the current-voltage-characteristic of a diode (cf. Sections 4.2 and 4.3). By plotting the intensity of light against its wavelength, one is able to determine the wavelength corresponding to a maximum intensity. The plot is shown in fig. 2, where some data is omitted for the sake of clarity.

By examining the intensity distribution we were able to determine the wavelengths corresponding to maxima of intensity as well as estimating their uncertainty based on the relative width of the intensity curve. Our estimates of the wavelengths maximizing the intensity are given in table 2 and are marked in the plot above. Because some wavelengths featured a wider spectrum a higher error was estimated.

Diode label	Wavelength in nm
380	380 ± 3
410	414 ± 3
430	430 ± 3
490	501 ± 3
515	523 ± 4
658	654 ± 3

Table 2: Measurement from the wavelengths of the used diodes

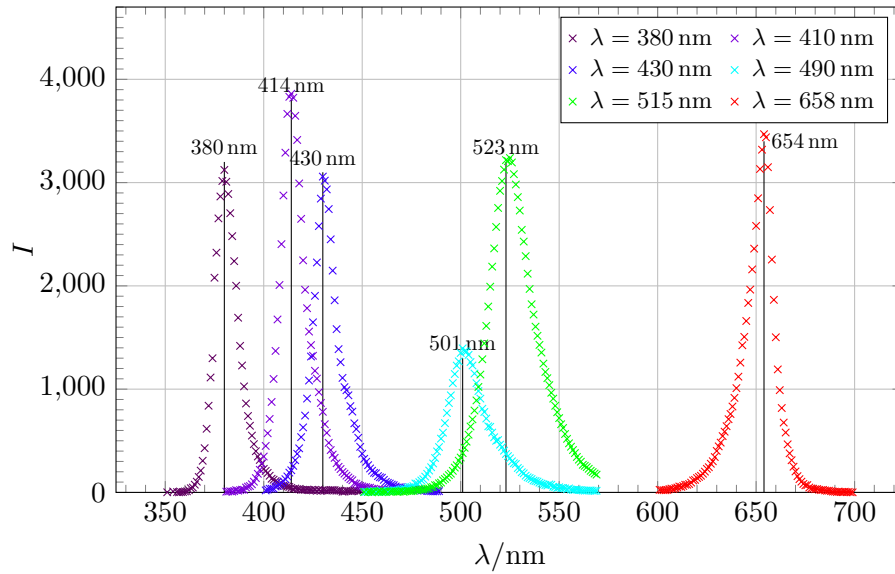


Figure 2: Intensity distribution of light emitted by various diodes

5.2 Current-Voltage Characteristic of a Diode for Different Intensities

From our measurements of the photo current for different reverse voltages between -4 V and 4 V we were able to obtain the plot shown in fig. 3 for the three different diodes analyzed with a current-fault circuit. As it isn't required, the current fault was not corrected in the creation of the plot.

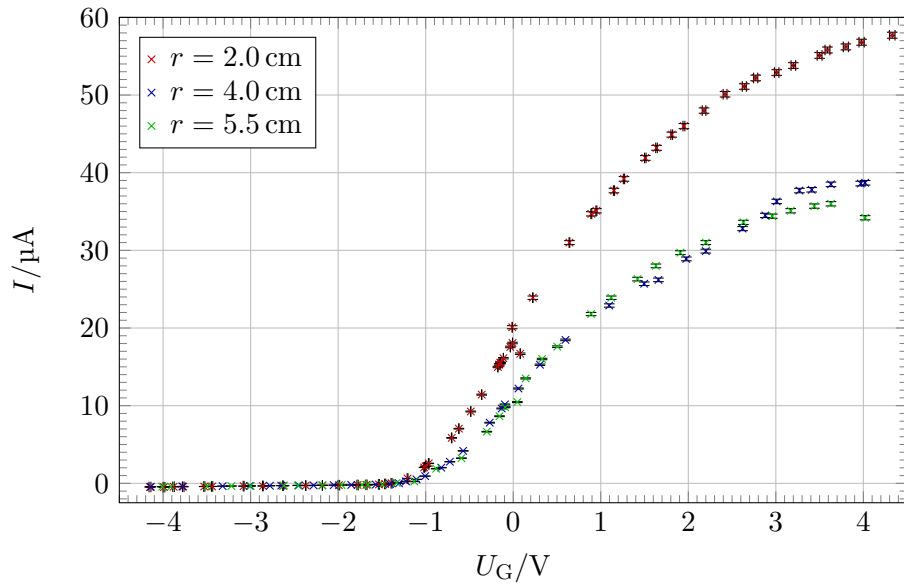


Figure 3: Current-voltage characteristic for a distance of 2 cm, 4 cm, and 5.5 cm in a current-fault circuit between photo cell and diode

To compare our measurements by use of the current-fault circuit with the voltage-fault circuit we plotted the photo current measured with the current-fault circuit at $r = 2$ cm along the photo current measured using the voltage-fault circuit at the same distance using the same diode. The plot can be seen in fig. 4. As for the different circuits, no correction regarding current or voltage fault was taken.

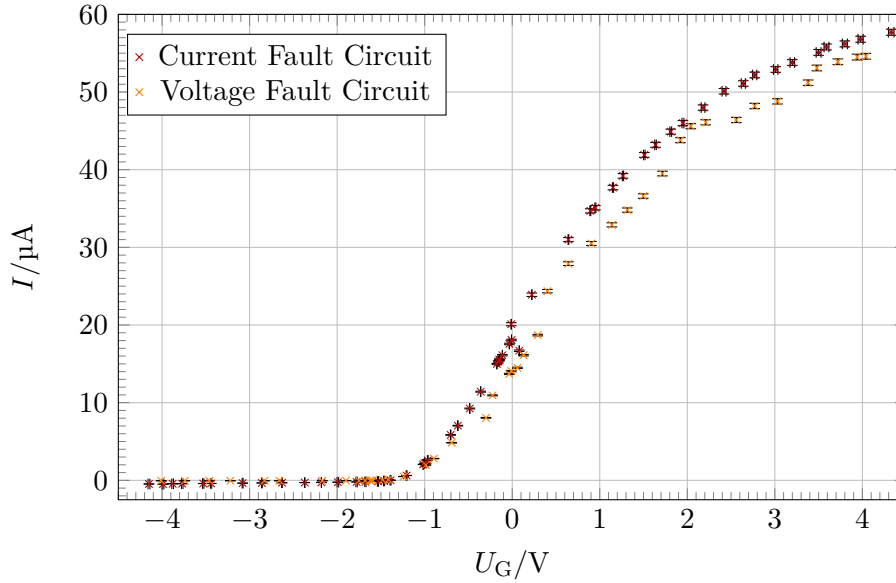


Figure 4: Current-voltage characteristic for a distance of 2 cm between photo cell and diode in a voltage-fault circuit

5.3 Current-Voltage Characteristic for Different Frequencies and Determination of the reverse voltage

In this part of the analysis the maximum reverse voltage $U_{G,\max}$ is to be determined for the wavelengths of the five diodes listed in section 4.2. Before we can do further calculations, the photo current has to be extracted from the faulty current we measured. Because some current flows through the voltmeter and not through the photo cell, the measured current is slightly higher than the photo current. This can be corrected by use of Ohm's law on the voltmeter: With an internal resistance [2] of $R_V = 10 \text{ M}\Omega$ one can calculate the current flowing through the voltmeter using

$$I_V = \frac{U_G}{R_V}. \quad (7)$$

Assuming the internal resistance as an exact value, the error on the voltmeter current is

$$s_{I_V} = \frac{s_{U_G}}{R_V}. \quad (8)$$

The photo current can then be calculated simply by subtracting the current flowing through the voltmeter from the measured current:

$$I_{\text{ph}} = I - I_V \quad (9)$$

The error on the photo current can then be calculated by use of the Gaussian error propagation:

$$s_{I_{\text{ph}}} = \sqrt{s_I^2 + s_{I_V}^2} \quad (10)$$

Applying the procedure described above for each value of the measured voltage, we can now proceed to calculate the maximum reverse voltage.

Because the photo current is proportional to the square of the respective energy as shown in eq. (5), the square root of the photo current has been plotted against the reverse voltage in order to find the maximum voltage where no photo current can be measured anymore. While the error on the voltage obviously doesn't change, the error on the square root of the photo current can be estimated through Gaussian error propagation as follows:

$$s_{\sqrt{I_{\text{ph}}}} = \frac{s_{I_{\text{ph}}}}{2\sqrt{I_{\text{ph}}}} \quad (11)$$

Now the square root of the photo current can be plotted against the reverse voltage U_G in order to find the maximum reverse voltage. This is done in figs. 5 to 9.

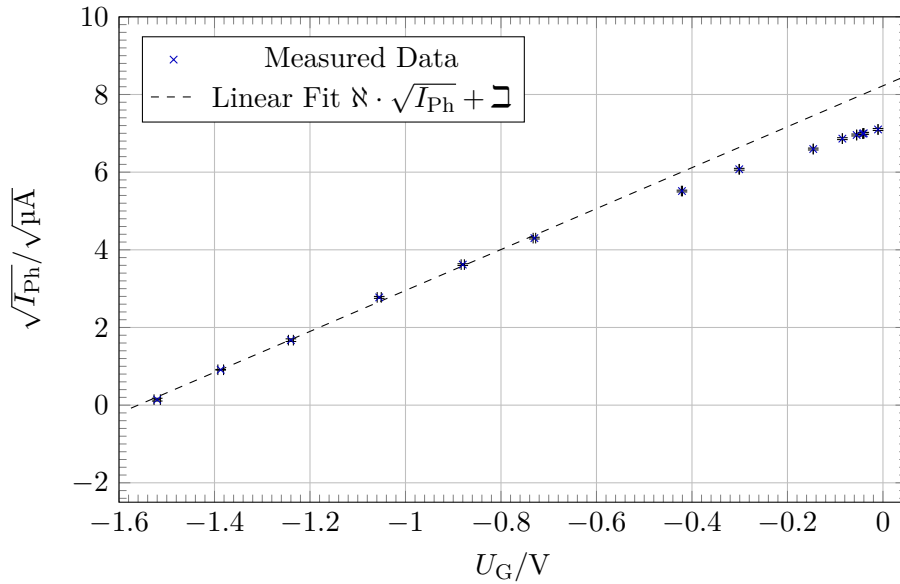


Figure 5: Current-voltage characteristic for diode with light of a wavelength of $\lambda = (380 \pm 3) \text{ nm}$

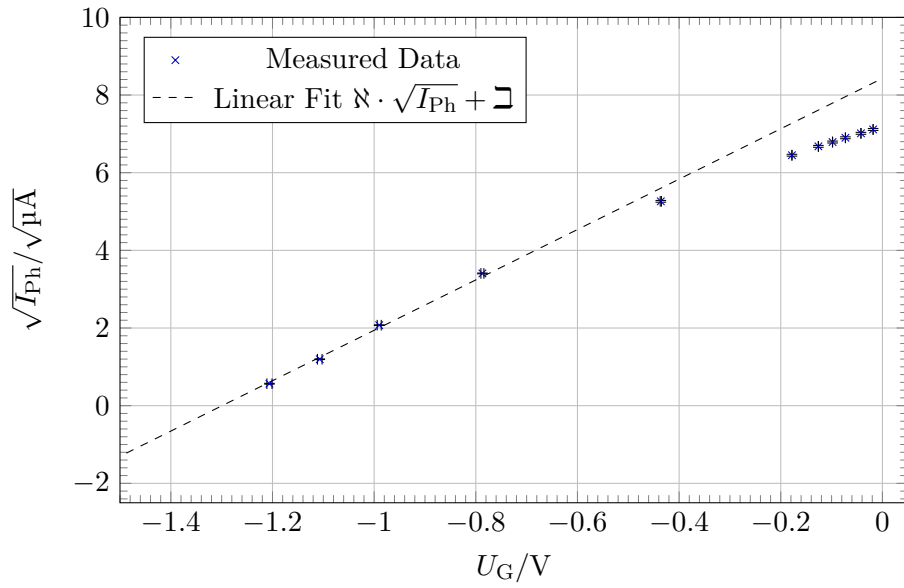


Figure 6: Current-voltage characteristic for diode with light of a wavelength of $\lambda = (430 \pm 3)$ nm

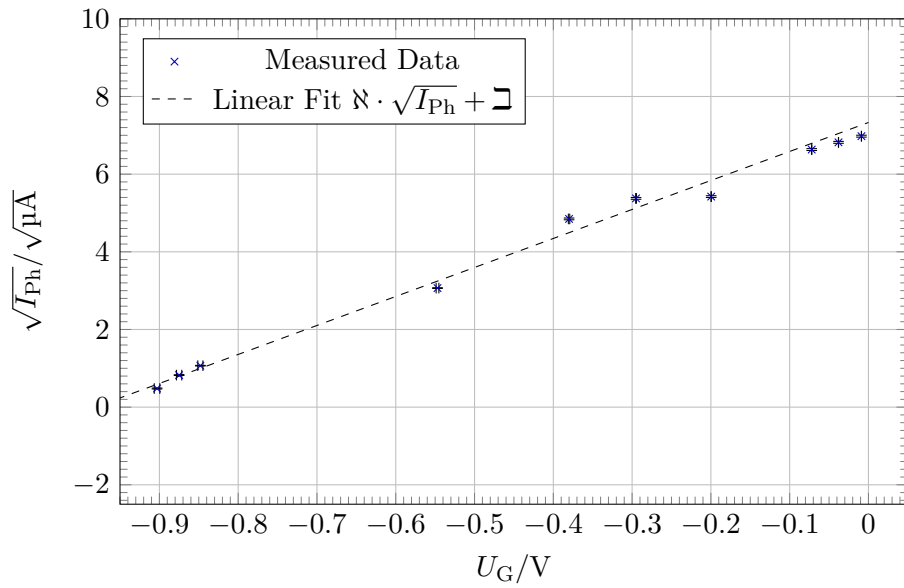


Figure 7: Current-voltage characteristic for diode with light of a wavelength of $\lambda = (523 \pm 4)$ nm

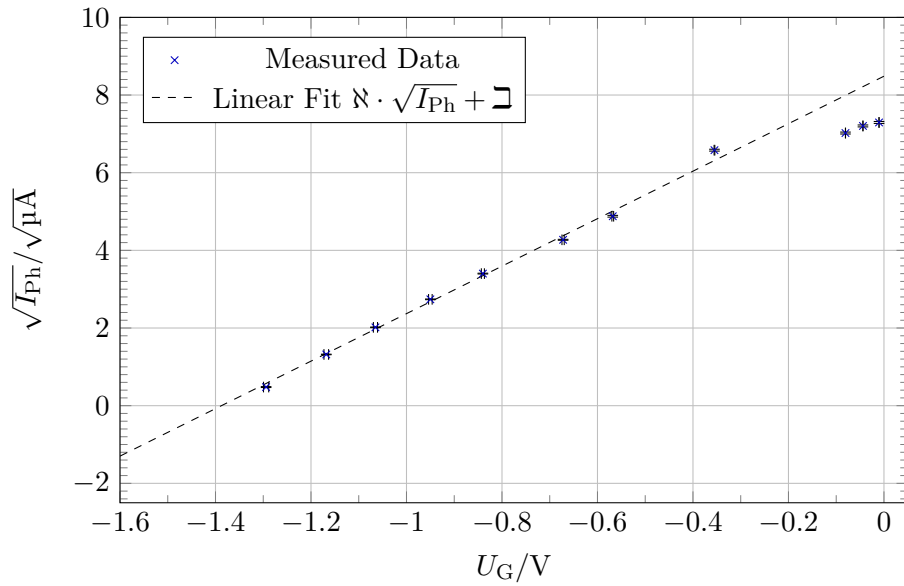


Figure 8: Current-voltage characteristic for diode with light of a wavelength of $\lambda = (410 \pm 3) \text{ nm}$

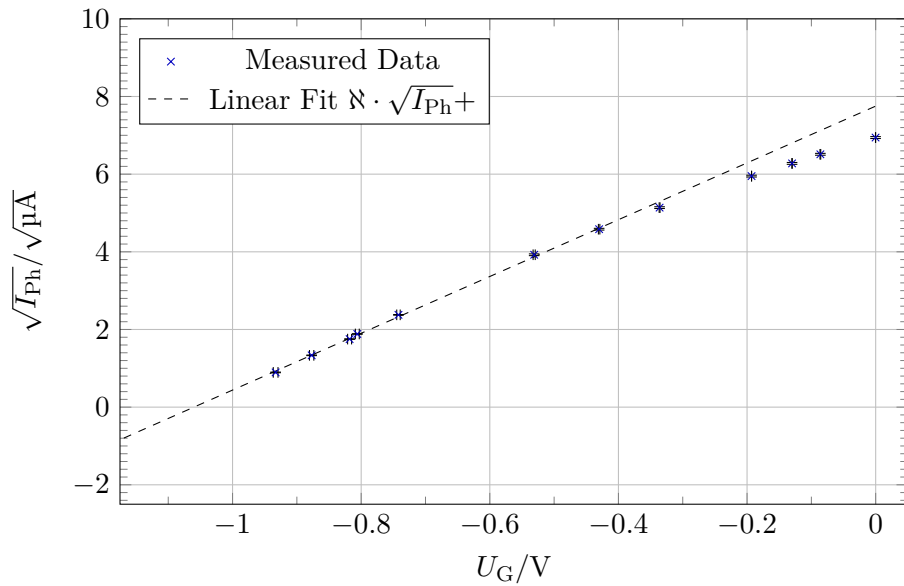


Figure 9: Current-voltage characteristic for diode with light of a wavelength of $\lambda = (501 \pm 3) \text{ nm}$

In addition to the raw data a line of best fit is shown in figs. 5 to 9. Each line is a result of a linear regression using the least-squares estimator for a

linear model (cf. appendix A.1) of the form

$$\sqrt{I_{\text{ph}}} = \aleph \cdot U_{\text{G}} + \beth, \quad (12)$$

where \aleph and \beth are parameters to be determined by the linear regression. As input values we chose to limit ourselves to values of $\sqrt{I_{\text{ph}}}$ closest to the U_{G} -Axis as we suspect a higher influence of systematic errors with increasing voltage. With \aleph and \beth determined for each diode one can calculate the intersect with the U_{G} -Axis using

$$U_{\text{G,max}} = -\frac{\beth}{\aleph}. \quad (13)$$

The error on $U_{\text{G,max}}$ can also be estimated by application of gaussian error propagation:

$$s_{U_{\text{G,max}}} = \sqrt{\left(\frac{s_{\beth}}{\aleph}\right)^2 + \left(\frac{\beth}{\aleph^2} s_{\aleph}\right)^2} \quad (14)$$

The maximum reverse voltage of each diode is shown alongside the parameters of linear regression used for calculation in table 3. In addition to the quantities described above one can find the frequency ν associated with each wavelength λ in the table. This was calculated using

$$\nu = \frac{c_0}{\lambda}, \quad (15)$$

where $c_0 = 299\,792\,458 \frac{\text{m}}{\text{s}}$ is the speed of light in a vacuum [1]. The error on ν can once again be found by use of gaussian error propagation:

$$s_{\nu} = \frac{c_0}{\lambda^2} s_{\lambda} \quad (16)$$

The frequency ν can be found in table 3 as was mentioned before.

λ in nm	ν in Hz	\aleph in $\frac{\sqrt{\mu\text{A}}}{\text{V}}$	\beth in $\sqrt{\mu\text{A}}$	$U_{\text{G,max}}$ in V
380 ± 3	7.89×10^{14}	5.271 ± 0.028	8.22 ± 0.03	1.560 ± 0.011
410 ± 3	7.24×10^{14}	6.488 ± 0.024	8.429 ± 0.025	1.388 ± 0.005
430 ± 3	6.97×10^{14}	7.467 ± 0.024	7.331 ± 0.019	1.299 ± 0.006
501 ± 3	5.98×10^{14}	6.115 ± 0.019	8.485 ± 0.020	1.060 ± 0.005
523 ± 4	5.73×10^{14}	7.313 ± 0.027	7.752 ± 0.023	0.982 ± 0.004

Table 3: Determination of the reverse voltage for different diodes

5.4 Determination of the Planck Constant

Now that we found the maximum reverse voltages $U_{\text{G,max}}$ for all diodes the planck constant h can be determined: One can see from eq. (4) that if we

plot the maximum reverse voltage w. r. t. the frequency of the incoming light, we expect to see a linear relation between the voltage $U_{G,\max}$ and the frequency ν . In particular, the slope of the line corresponds to the planck constant h multiplied by the elementary charge e , while the axis intersect equates to the anode work function ϕ_A . In order to proceed, we plot the voltage w. r. t. the frequencies from table 3 in the diagram shown in fig. 10.

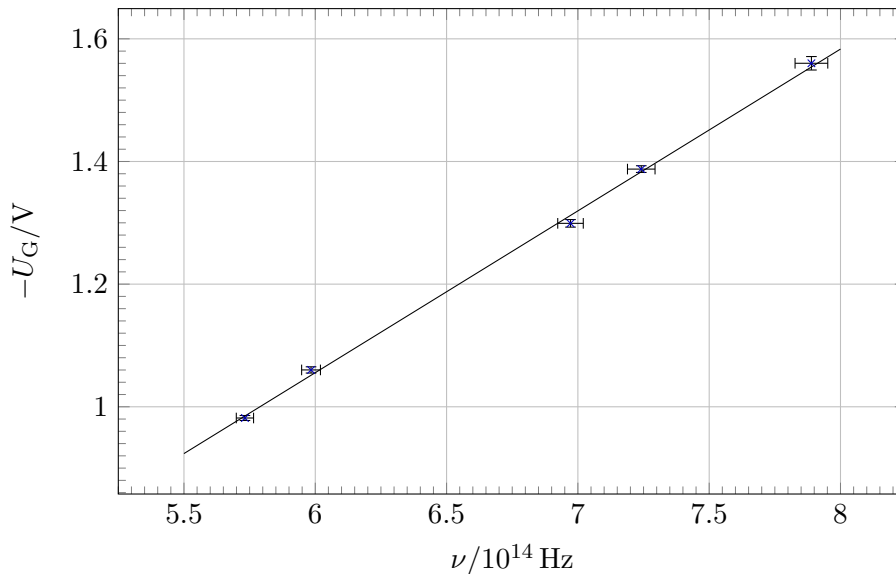


Figure 10: Maximum reverse voltages $U_{G,\max}$ and their corresponding frequencies ν extracted from table 3.

As we can see in the figure, the error on the frequency is – relatively speaking – vastly higher than the error on the reverse voltage. This poses a problem for the use of a linear regression, as the least-squares estimator assumes the independent variable to be known exactly. We can circumvent² this problem by choosing the maximum reverse voltage $U_{G,\max}$ to be the independent variable, i. e. instead of using a model of the form

$$U_{G,\max} = \aleph \cdot \nu + \beth, \quad (17)$$

where \aleph and \beth are parameters of regression, we conduct a regression of the form

$$\nu = \beth \cdot U_{G,\max} + \beth, \quad (18)$$

where \beth and \beth , too are parameters of regression and relate to \aleph and \beth by

$$\aleph = \beth^{-1} \quad \text{and} \quad \beth = -\frac{\beth}{\beth}. \quad (19)$$

²While this method certainly doesn't address the errors of all variables, it is an improvement over determining \aleph and \beth (defined in eq. (17)) directly.

By the use of error propagation we find the errors on \aleph and \beth :

$$\begin{aligned} s_{\aleph} &= \frac{s_{\beth}}{\beth^2}, \\ s_{\beth} &= \sqrt{\left(\frac{s_{\beth}}{\beth}\right)^2 + \left(\frac{\beth}{\beth^2} s_{\beth}\right)^2}. \end{aligned} \quad (20)$$

With our values from table 3 and using eqs. (17) to (20) we conduct a linear regression and obtain:

$$\begin{aligned} \beth &= (-3.79 \pm 0.10) \times 10^{15} \frac{\text{Hz}}{\text{V}} \\ \beth &= (2.0 \pm 1.1) \times 10^{15} \text{ Hz} \\ \aleph &= (-2.64 \pm 0.07) \times 10^{-15} \frac{\text{V}}{\text{Hz}} \\ \beth &= (-0.528 \pm 0.003) \text{ V} \end{aligned} \quad (21)$$

According to eq. (4), the planck constant can then be calculated simply by multiplication of the elementary charge e , which we assume to be exactly [1] $e = 1.602 \times 10^{-19} \text{ C}$:

$$h_{\text{calc}} = -\aleph \cdot e = (4.2 \pm 0.5) \times 10^{-34} \text{ Js} \quad (22)$$

The work function ϕ_A can be calculated in the same way:

$$\phi_A = -\beth \cdot e = (8.46 \pm 0.06) \times 10^{-20} \text{ J}. \quad (23)$$

6 Discussion

6.1 Determination of the Wavelengths from the Diodes

Out of our measurements we determined the wavelengths in table 4 for the different diodes.

Diode label	Wavelength in nm
380	380 ± 3
410	414 ± 3
430	430 ± 3
490	501 ± 3
515	523 ± 4
658	654 ± 3

Table 4: Measurement from the wavelengths of the used diodes

As was mentioned before, the intensity distribution shown on the laptop was constantly changing and our hands aren't perfectly steady. So there could be the possibility that that we misjudged the statistical error on the wavelengths and therefore estimated it as too low.

6.2 Current-Voltage Characteristic of a Diode for Different Intensities

On the one hand one can see in fig. 3 that the smaller the distance r between the diodes becomes, the higher the magnitude of the photo current gets. On the other hand one can observe, that the maximum reverse voltage (i. e. the approximate location of the x -axis intersect) is independent of the distance and therefore the intensity, because the photo current reaches the level of zero A at the same point for all different intensities of light.

In addition one can make out of fig. 3 that the distance between the curve belonging to the distance $r = 5.5$ cm and the curve of $r = 4.4$ cm is noticeably smaller than the distance between the curve of $r = 4.4$ cm and $r = 2$ cm. This fits our expectations of the relation shown in eq. (6), which states that the intensity is inversely proportional to the square of the distance r : As we can see from

$$\frac{1/2^2}{1/4^2} = 4 > 1.890625 = \frac{1/4^2}{1/5.5^2}, \quad (24)$$

the relative change from $r = 2$ cm to 4 cm has a much larger impact on the intensity than the relative change from $r = 4$ cm to 5.5 cm.

In fig. 4 one can see that all measured values by use of the voltage-fault circuit are a bit lower than the measured values by use of the current-fault circuit. The reason for this is that the value of the current in the current-fault circuit is constantly higher than its value in the voltage-fault circuit, because the ampere-meter additionally picks up the current flowing through the voltmeter. Using a voltage-fault circuit instead results in a higher voltage being measured by the voltmeter, such that the curve gets stretched out in the x -direction.

We decided to use the current-fault circuit for our measurements, because we wanted to determine the planck constant as exactly as possible. As the reverse voltage plays a huge part in determining the maximum stopping voltage and therefore the planck constant h instead, it seems reasonable to assume that one wants to know the voltage to a reasonable high degree.

6.3 Current-Voltage Characteristic for Different Frequencies and Determination of the reverse voltage

In this part of the experiment we determined the reverse voltages for different diodes and obtained the voltages in table 5.

λ in nm	ν in Hz	\aleph in $\frac{\sqrt{\mu\text{A}}}{\text{V}}$	\beth in $\sqrt{\mu\text{A}}$	$U_{G,\text{max}}$ in V
380 ± 3	7.89×10^{14}	5.271 ± 0.028	8.22 ± 0.03	1.560 ± 0.011
410 ± 3	7.24×10^{14}	6.488 ± 0.024	8.429 ± 0.025	1.388 ± 0.005
430 ± 3	6.97×10^{14}	7.467 ± 0.024	7.331 ± 0.019	1.299 ± 0.006
501 ± 3	5.98×10^{14}	6.115 ± 0.019	8.485 ± 0.020	1.060 ± 0.005
523 ± 4	5.73×10^{14}	7.313 ± 0.027	7.752 ± 0.023	0.982 ± 0.004

Table 5: Determination of the reverse voltage for different diodes

In figs. 5 to 9 one can see the expected linear course from the square root of the photo current plotted against the reverse voltage. But we should mention that we have to account statistical errors concerning the measuring of the photo current and the voltage. Especially in small measuring ranges of the multimeter the fluctuation of the measured values of the photo current were not to be dismissed.

As the data points near the axis intersect seem to fit a linear model a bit better than values for the square root of the photo current at a higher distance from the axis, we conducted the linear regression to find the maximum stopping voltage only using data near the axis intersect. We justified this by saying that a potential systematic error dependent on the current gets more relevant for higher values of the photo current and as such skews higher data points more. As we don't know the exact bearings used to derive eq. (5), it is ill-advised to count on those values as we can't exactly make out a linear relation accounting them. Nonetheless, the possibility of a gross error in the data analysis shouldn't be dismissed at this point.

6.4 Determination of the Planck Constant

After applying the in table 5 determined values of the reverse voltage on their frequencies in fig. 10, we could determine the values for h and ϕ_A including their uncertainties with a linear regression and got the values:

$$h_{\text{calc}} = (4.23 \pm 0.11) \times 10^{-34} \text{ Js} \quad (25)$$

for the Planck constant and for the work function

$$\phi_A = (8.46 \pm 0.06) \times 10^{-20} \text{ J}. \quad (26)$$

The literature value [1] of the Planck constant is

$$h_{\text{lit}} = 6.626 \times 10^{-34} \text{ Js}. \quad (27)$$

The deviation between the literature value and the calculated value of the Planck constant is about 22 σ -environments. This means that the statistical error on our measurements is far too small. The reason for this could be

that we misjudged the statistical error of the wavelengths (which seem to make out a great part in the error of the end result) as not big enough. It may also result out of the linear regression, because by making a linear regression in the way we did one assumes that there is no uncertainty on the x -value. The deviation between the values for the Planck constant may also result out of a systematic error: As one can see in fig. 10, the line fits the underlying data within error quite well. A systematic error doesn't therefore seem far fetched. As we can see from comparing the literature value and the value we obtained, in order for our value to be correct, the line in fig. 10 has to have a higher slope, meaning that the systematic error would need to depend on the maximum reverse voltages. It is therefore entirely possible that by neglecting values far from the x -Axis in section 5.3, we miscalculated the maximum reverse voltages resulting in a way lower Planck constant h . A systematic error like this which scales with the voltage can also be caused by a miscalibrated multimeter: If the voltage was multiplied by a constant factor, the slope in fig. 10 would be affected accordingly.

The error can also be caused of external light influences (we didn't work in a darkened room) or temperature fluctuations. In addition we should note that we assumed that the value of the internal resistance of the voltmeter is exact and that we should have accounted additional internal resistances of the diodes or of the used wires.

A Appendix

A.1 Linear Regression

In this section we show our method of conducting a linear regression. Assuming some expected linear relation between the quantities x and y of the form

$$y = \aleph \cdot x + \beth, \quad (28)$$

and some underlying observations $(x_i, y_i \pm s_{y_i})$, where the x_i 's are known to a high degree, the method of least squares yields the following estimators:

$$\begin{aligned} \hat{\aleph} &= \frac{\sum g_i x_i^2 \sum g_i y_i - \sum g_i x_i \sum g_i x_i y_i}{\sum g_i \sum g_i x_i^2 - (\sum g_i x_i)^2} \\ \hat{\beth} &= \frac{\sum g_i \sum g_i x_i y_i - \sum g_i x_i \sum g_i y_i}{\sum g_i \sum g_i x_i^2 - (\sum g_i x_i)^2} \end{aligned} \quad (29)$$

The weights g_i are defined to be $g_i = s_{y_i}^2$. All sums are to be understood to be starting at $i = 1$ and ending at n . One can express the errors on the

estimators $\hat{\kappa}$ and $\hat{\mu}$ in the following way:

$$\begin{aligned} s_{\hat{\kappa}} &= \sqrt{\frac{\sum g_i}{\sum g_i \sum g_i x_i^2 - (\sum g_i x_i)^2}} \\ s_{\hat{\mu}} &= \sqrt{\frac{\sum g_i x_i^2}{\sum g_i \sum g_i x_i^2 - (\sum g_i x_i)^2}} \end{aligned} \tag{30}$$

A.2 Lab Notes

Handwritten lab notes on a grid background, titled "Versuch 8 - Geometrie, 2000". The notes include a table with columns for "Einde", "m", "n", "m+n", "m-n", and "m/n". The table contains numerical data points, some with handwritten annotations like "Abstand 5,5cm", "Abstand 4cm", and "Abstand 3cm".

Handwritten notes: "Abstand 5,5cm", "Abstand 4cm", "Abstand 3cm".

Einde	m	n	m+n	m-n	m/n
1	1	1	2	0	1
2	2	1	3	1	2
3	3	1	4	2	3
4	4	1	5	3	4
5	5	1	6	4	5
6	6	1	7	5	6
7	7	1	8	6	7
8	8	1	9	7	8
9	9	1	10	8	9
10	10	1	11	9	10
11	11	1	12	10	11
12	12	1	13	11	12
13	13	1	14	12	13
14	14	1	15	13	14
15	15	1	16	14	15
16	16	1	17	15	16
17	17	1	18	16	17
18	18	1	19	17	18
19	19	1	20	18	19
20	20	1	21	19	20
21	21	1	22	20	21
22	22	1	23	21	22
23	23	1	24	22	23
24	24	1	25	23	24
25	25	1	26	24	25
26	26	1	27	25	26
27	27	1	28	26	27
28	28	1	29	27	28
29	29	1	30	28	29
30	30	1	31	29	30
31	31	1	32	30	31
32	32	1	33	31	32
33	33	1	34	32	33
34	34	1	35	33	34
35	35	1	36	34	35
36	36	1	37	35	36
37	37	1	38	36	37
38	38	1	39	37	38
39	39	1	40	38	39
40	40	1	41	39	40
41	41	1	42	40	41
42	42	1	43	41	42
43	43	1	44	42	43
44	44	1	45	43	44
45	45	1	46	44	45
46	46	1	47	45	46
47	47	1	48	46	47
48	48	1	49	47	48
49	49	1	50	48	49
50	50	1	51	49	50
51	51	1	52	50	51
52	52	1	53	51	52
53	53	1	54	52	53
54	54	1	55	53	54
55	55	1	56	54	55
56	56	1	57	55	56
57	57	1	58	56	57
58	58	1	59	57	58
59	59	1	60	58	59
60	60	1	61	59	60
61	61	1	62	60	61
62	62	1	63	61	62
63	63	1	64	62	63
64	64	1	65	63	64
65	65	1	66	64	65
66	66	1	67	65	66
67	67	1	68	66	67
68	68	1	69	67	68
69	69	1	70	68	69
70	70	1	71	69	70
71	71	1	72	70	71
72	72	1	73	71	72
73	73	1	74	72	73
74	74	1	75	73	74
75	75	1	76	74	75
76	76	1	77	75	76
77	77	1	78	76	77
78	78	1	79	77	78
79	79	1	80	78	79
80	80	1	81	79	80
81	81	1	82	80	81
82	82	1	83	81	82
83	83	1	84	82	83
84	84	1	85	83	84
85	85	1	86	84	85
86	86	1	87	85	86
87	87	1	88	86	87
88	88	1	89	87	88
89	89	1	90	88	89
90	90	1	91	89	90
91	91	1	92	90	91
92	92	1	93	91	92
93	93	1	94	92	93
94	94	1	95	93	94
95	95	1	96	94	95
96	96	1	97	95	96
97	97	1	98	96	97
98	98	1	99	97	98
99	99	1	100	98	99
100	100	1	101	99	100

Sportplatz - Situation		Fläche 390		Tafel	
1. Standort 2007		2. Standort 2008		3. Standort	
U	I	U	I	U	I
3,00	20	3,00	20	3,00	20
3,10	20	3,10	20	3,10	20
3,20	20	3,20	20	3,20	20
3,30	20	3,30	20	3,30	20
3,40	20	3,40	20	3,40	20
3,50	20	3,50	20	3,50	20
3,60	20	3,60	20	3,60	20
3,70	20	3,70	20	3,70	20
3,80	20	3,80	20	3,80	20
3,90	20	3,90	20	3,90	20
4,00	20	4,00	20	4,00	20
4,10	20	4,10	20	4,10	20
4,20	20	4,20	20	4,20	20
4,30	20	4,30	20	4,30	20
4,40	20	4,40	20	4,40	20
4,50	20	4,50	20	4,50	20
4,60	20	4,60	20	4,60	20
4,70	20	4,70	20	4,70	20
4,80	20	4,80	20	4,80	20
4,90	20	4,90	20	4,90	20
5,00	20	5,00	20	5,00	20
5,10	20	5,10	20	5,10	20
5,20	20	5,20	20	5,20	20
5,30	20	5,30	20	5,30	20
5,40	20	5,40	20	5,40	20
5,50	20	5,50	20	5,50	20
5,60	20	5,60	20	5,60	20
5,70	20	5,70	20	5,70	20
5,80	20	5,80	20	5,80	20
5,90	20	5,90	20	5,90	20
6,00	20	6,00	20	6,00	20
6,10	20	6,10	20	6,10	20
6,20	20	6,20	20	6,20	20
6,30	20	6,30	20	6,30	20
6,40	20	6,40	20	6,40	20
6,50	20	6,50	20	6,50	20
6,60	20	6,60	20	6,60	20
6,70	20	6,70	20	6,70	20
6,80	20	6,80	20	6,80	20
6,90	20	6,90	20	6,90	20
7,00	20	7,00	20	7,00	20
7,10	20	7,10	20	7,10	20
7,20	20	7,20	20	7,20	20
7,30	20	7,30	20	7,30	20
7,40	20	7,40	20	7,40	20
7,50	20	7,50	20	7,50	20
7,60	20	7,60	20	7,60	20
7,70	20	7,70	20	7,70	20
7,80	20	7,80	20	7,80	20
7,90	20	7,90	20	7,90	20
8,00	20	8,00	20	8,00	20
8,10	20	8,10	20	8,10	20
8,20	20	8,20	20	8,20	20
8,30	20	8,30	20	8,30	20
8,40	20	8,40	20	8,40	20
8,50	20	8,50	20	8,50	20
8,60	20	8,60	20	8,60	20
8,70	20	8,70	20	8,70	20
8,80	20	8,80	20	8,80	20
8,90	20	8,90	20	8,90	20
9,00	20	9,00	20	9,00	20
9,10	20	9,10	20	9,10	20
9,20	20	9,20	20	9,20	20
9,30	20	9,30	20	9,30	20
9,40	20	9,40	20	9,40	20
9,50	20	9,50	20	9,50	20
9,60	20	9,60	20	9,60	20
9,70	20	9,70	20	9,70	20
9,80	20	9,80	20	9,80	20
9,90	20	9,90	20	9,90	20
10,00	20	10,00	20	10,00	20

f_0	f_1	f_2	f_3
-110	170	220	270
-100		240	
-90		40	
-80	20	100	
-70		180	
-60		260	
-50		340	
-40		420	
-30		500	
-20		580	
-10		660	
0		740	
10		820	
20		900	
30		980	
40		1060	
50		1140	
60		1220	
70		1300	
80		1380	
90		1460	
100		1540	
110		1620	
120		1700	
130		1780	
140		1860	
150		1940	
160		2020	
170		2100	
180		2180	
190		2260	
200		2340	
210		2420	
220		2500	
230		2580	
240		2660	
250		2740	
260		2820	
270		2900	
280		2980	
290		3060	
300		3140	
310		3220	
320		3300	
330		3380	
340		3460	
350		3540	
360		3620	
370		3700	
380		3780	
390		3860	
400		3940	
410		4020	
420		4100	
430		4180	
440		4260	
450		4340	
460		4420	
470		4500	
480		4580	
490		4660	
500		4740	
510		4820	
520		4900	
530		4980	
540		5060	
550		5140	
560		5220	
570		5300	
580		5380	
590		5460	
600		5540	
610		5620	
620		5700	
630		5780	
640		5860	
650		5940	
660		6020	
670		6100	
680		6180	
690		6260	
700		6340	
710		6420	
720		6500	
730		6580	
740		6660	
750		6740	
760		6820	
770		6900	
780		6980	
790		7060	
800		7140	
810		7220	
820		7300	
830		7380	
840		7460	
850		7540	
860		7620	
870		7700	
880		7780	
890		7860	
900		7940	
910		8020	
920		8100	
930		8180	
940		8260	
950		8340	
960		8420	
970		8500	
980		8580	
990		8660	
1000		8740	

Handwritten notes in red ink: "UT: 11/20/2023 M. 10:15"

References

- [1] MESCHEDE, Dieter: *Gerthsen Physik*. Springer Verlag, 2010. – 1 S.
- [2] UNI-TREND TECHNOLOGY LTD.: *Model UT51-55: Operating Manual*. <http://www.ageta.hu/pdf/UT51-55.pdf>. – [Online; accessed 28-March-2019]